Feasibility study on piezoelectric actuated automotive morphing wing

FEASIBILITY STUDY ON PIEZOELECTRIC ACTUATED AUTOMOTIVE MORPHING WING

Alessandro Messana
Politecnico di Torino - Italy

Lorenzo Sisca
Politecnico di Torino - Italy

Henrique De Carvalho Pinheiro
Politecnico di Torino - Italy

Davide Berti Polato
Beond s.r.l. Torino - Italy

Alessandro Ferraris
Beond s.r.l. Torino - Italy

Andrea Giancarlo Airale
Beond s.r.l. Torino - Italy

Massimiliana Carello
Politecnico di Torino - Italy

Abstract
Active aerodynamics is a promising technology to improve vehicle performance and efficiency, but so far in the automotive field the actuation methods suffer with several drawbacks that jeopardize its functioning and broad implementation. Morphing wings represent a technology already studied for aerospace applications that could help overcoming some of those issues. This paper proposes a piezoelectric transducer actuation for a composite material automotive wing and seeks to validate it through virtual models and physical tests. Experimental validation with a 3D-printed simplified wing profile confirms the feasibility of the technology and helps determining the best position for the piezo actuator. Furthermore, a FEM model is presented, where the piezo effect is simulated through a thermal analogy. An optimization of the composite stacking sequence is performed to maximize the trailing edge displacements, and its results are compared with the deflection caused by aerodynamic loads observed in the wing. The displacement of the trailing edge is in the order of tenths of a millimeter, even though further investigations are necessary to improve overall impact of the solution the preliminary results are promising.

Nomenclature
AOA – Angle of Attack
CAD - Computer Aided Design
CD- Drag Coefficient
DRS – Drag Reduction System
DLP - Direct Light Projection
FE – Finite Element
FEM - Finite Element Method
MFC – Macro Fiber Composite
SMA- Shape Memory Alloys
TE – Trailing Edge

INTRODUCTION

The automotive industry and technologies are evolving towards a sustainable and emission free future especially due to new environmental regulations and targets [1]. Being the electrification one of the trendiest topics nowadays [2], automotive companies invest a lot of their efforts to reduce the fuel/energy consumption and thus to the aerodynamic efficiency of the cars. Furthermore, the study of the aerodynamics provides new direction to the designers of future generations cars. For example, a 0,01 reduction of the drag coefficient corresponds to 0,85 kilometers per liter improvement in fuel economy [3]. Reducing the generated drag will allow a vehicle to travel for longer distance with same amount of fuel or to equip it whit a smaller battery that favors a cheaper car and an overall mass reduction. Up to now, regarding road vehicles, every aerodynamic appendix was a fixed device which was able to provide improvements either to the cooling system or to the drag reduction, sometimes reducing the lift generation of the vehicle [4-7]. Regarding sports and racing cars, there can be seen some models including active aerodynamic systems that allow to manipulate air to their benefit but, in any case, their actuation system consisted of mechanic, pneumatic or hydraulic system electronically activated. For this reason, the aim of this paper is a feasibility analysis on the design of an active wing (also called morphing wing) actuated by a piezoelectric system to evaluate a future automotive application, that include racing and urban vehicles. The novelty of this concept consists in a lightweight technology adopted to actuate the wing without using heavy traditional electric or hydraulic systems: the piezoelectric patch can be integrated even inside the component during the manufacturing process especially for wing made of composite materials.

A prototype wing has been made of plastic through additive manufacturing process and the material used has been experimentally characterized to be correlated with FEM simulations. Then, two different piezo configurations have been experimentally tested to carry out the best position along the wing surfaces. Subsequently, a finite element simulation has been conducted to calibrate the piezoelectric virtual model by correlating it with the experimental test. Then, a first virtual model of a carbon fiber morphing wing

section has been designed to estimate the piezoelectric system performance. In this case, a fluid-dynamic simulation has been carried out to consider the aerodynamic load effects.
Finally, the results discussion highlights the pros and cons regarding this first-stage technology application.

ACTIVE AERODYNAMICS SCENARIO

Active aerodynamic is by now among best practices for sports and super cars. There are plenty examples of high segment cars and motorsport racing in which a wing can vary its height or angle of attack, granting a more adequate performance for each driving situation. By varying the aerodynamic set-up, the car can achieve a balance between efficiency and road holding ability but on a more limited way than changing its geometrical parameters such as camber, span or thickness.
The necessity to vary continuously the wing contribution is due to the different vehicle working conditions such as straight line, curve, and speed. For instance, in a straight line the wing must reduce drag to achieve the maximum speed possible while in curve it must generate the maximum downforce possible to increase tire grip. The most common solutions in automotive field consist in a discrete regulation of the following aerodynamic parameters: angle of attack, wing thickness and lateral wing inclination.
The most famous example is the active system adopted in formula 1 cars is the DRS showed in Figure 1 [8].

Figure 1 - Drag Reduction System in F1 car

It is a two-position hydraulic actuated system (active or disable) that vary the AOA of the rear wing upper flap reducing the aerodynamic drag of the vehicle. This effect is due to the gap increase between the main wing and the flap then a reduction of the airfoil camber line is obtained that cause a downforce and drag decrease.
Another application is the “Centripetal Wing” of the Zenvo TSR-S reported in Figure 2 [9]. The Centripetal Wing has two rotation degrees of freedom enabling it function as an air brake and cornering stabilizer. When the TSR-S corners the wing rotates around the car’s longitudinal direction generating an inward force together with the conventional downforce. This behavior boosts inner tire grip and cornering stability.

Figure 2 -The “Centripetal Wing” of the Zenvo TSR-S ACTUATED

MORPHING TECHNOLOGY AND ACTUATION SYSTEMS

The variation of a wing aerodynamics’ set-up can provide a balance between efficiency and road holding ability but on a more limited way than changing geometrical parameters such as camber, span or thickness. Morphing structures can achieve this goal, allowing more sophisticated wing shape integrating with also the styling requirements.

Most part of morphing wing literature is focused especially on aerospace field. For instance, FlexSys developed the morphing wing concept showed in Figure 3 [10].

Figure 3 - Skin deformation of FlexFoil wing

These morphing airplane wing has a variable geometry trailing and leading edges that allow a drag reduction in the range 5% to 12%. Moreover, it is expected a 2% to 11% fuel saving from its application. The FlexFoil™ control surface changes the camber of a wing during flight and permits discrete span-wise twist of the compliant edge at high response rates. Other significant aerospace application is represented by [11] in which are used MFC technologies to actuate wing prototypes.
Because consumption reduction and overall performance the main objectives also in automotive field, the morphing technologies could have a wide range of application on the external aerodynamics of the car and on the air management into the cooling systems [12]. Regarding high performance sport cars, the Aston Martin BR 003 uses the FlexFoil morphing technology actuated by SMA to increase the camber of the rear spoiler and thus the downforce generation on the rear axis, as shown in Figure 4 [13].

Figure 4 - Aston Martin BR003 SMA wing

Nevertheless, the most common actuation systems on cars are mechanic or hydraulic system electronically activated (Table 1).

Table 1 - Actuation system comparison

Characteristic	Pneumatic	Hydraulic	Electric
Position accuracy	Very difficult to achieve	Mid-stroke positioning needs additional components	Positioning and velocity allow synchronization
Load ratings	High load ratings	Extremely high load ratings	Depend on speed and positioning desired
Lifetime	Moderate, Easy to replace	Long with good maintenance	Long with good maintenance

Environmental	High noise levels	Fluid leaks and disposal	Minimal
Efficiency	Low	Low	High
Reliability	Excellent	Good	Good
Maintenance	High maintenance	High user-maintenance	Little to no maintenance
Purchase cost	Low costs	High costs	High costs
Operating cost	Moderate costs	High costs	Low costs
Maintenance cost	Low costs	High costs	Low costs

To permit the deformation of the wing shape while getting rid of the previously mentioned disadvantages that the actual actuation systems imply, the application of piezo actuators is under massive research [14-15] and even in testing phase for aerospace and automotive field.

PIEZO SENSORS AND AIRFOIL DEFINITION

Piezo components can transform displacement into an electrical voltage (making the material a load or displacement sensor) or they can transform electrical voltage into displacement by the inverse piezoelectric effect (making the material an actuator). It consists of changing the shape of the target structure by the deformation of the piezo material. As mentioned previously, this deformation is achieved by applying a voltage.

Using piezoelectric system, the actuator is integral with the skin, so the volume of the actuator is negligible. The power and control electronics can be placed somewhere independently, which improves the ability to strategically locate the volume and mass. The continuous mold-line curvature of the actuator is ideal for low Reynolds number applications and eliminates the drag due to separation at the hinge line for articulated controls.

These actuators are widely used in the so-called smart structures due to their high electromechanical coupling factors and excellent frequency response. Because the aim of this work is focused on the evaluation of piezoelectric actuation on automotive field, it has been chosen a simplified airfoil suitable for a vehicle application. For this reason, the NACA 6412 foil has been taken as reference although it does not present the overall best aerodynamic performance.

As concerns the piezoelectric device, the DuraAct P876-K015 has been chosen (as depicted in Figure 5) because of high versatility either for actuator or sensor application.

Figure 5 - DuraAct P876-K015

Principal feature for this class of devices is the ability to support deformations, without compromising correct operation in transmitting and acquiring electrical signals. As a result, DuraAct patches can be bonded to curved surfaces, differently from classic piezoceramics that break due to excessive strain. The piezo main characteristics are reported in Table 2.

Table 2 - Piezoelectric transducer specs

Transducer	DuraAct P876-K015
Operating Voltage	-250 to 1000 V
Dimensions	61x35x0,8 mm
Piezoceramic core height	200 µm
Capacitance	45 µF
Class of piezoceramic core	PIC 255
Dimension for active plate	40x9x0,2 mm

Flexible elastic external layers	KAPTON
Resonance frequency	150 kHz
Operating temperature range	-40° to 150° C
Mass	0,75 g

ACTIVITY WORKFLOW

The application of piezoelectric sensor to actuate an automotive aerodynamic component is analyzed because of strong diffusion of electric vehicles moved by high voltage. Because high voltage is needed to actuate the piezoelectric actuator, this could be an enabling technology which make possible the PZT actuation simply using part of energy already available on board.

One of the advantages of DuraAct transducers is the possibility to integrate them directly into the composite stacks, because they are as thin as a common pre-preg layer and compliant with composite manufacturing process.

Thus, to evaluate the feasibility of this application, a specific workflow has been followed as described below:

Airfoil prototyping (also called simulacrum) in plastic material by additive manufacturing;
Experimental evaluation of PZT position and its effect on TE;
FE analysis and correlation to calibrate PZT virtual patch;
FE simulation on composite airfoil with the same simulacrum geometry.

The facilities available in BeonD srl laboratory were used to print both the wing section component and the specimen needed to characterize the 3D printed material. In this way the material was fully tested to generate a correlated material card to predict the whole component behavior.

Thus, the same experimental test layout has been reproduced to validate the piezoelectric modelling approach on FEM simulation to obtain a reliable model used as reference. This step has been considered mandatory together with the sensor position investigation before starting with the composite wing simulation.

Finally, the feasibility check of this solution has been conducted by a virtual analysis on the composite airfoil. The four steps previously described are expanded and detailed in the following chapters.

AIRFOIL MANUFACTURING AND piezo TESTING

A first airfoil prototype has been built in additive manufacturing by using the DLP technology and Formlabs Form2 machine at BeonD srl laboratory.

According to the printing machine volume, it has been produced a small section of the NACA 6412 with the same wing proportion but with a depth of 16 mm that means 1/111 of the real component. Other characteristics and size are:

Thickness: 1 mm
Chord: 165 mm
Depth: 16 mm
Trailing Edge fillet of 2.5 mm as standards [10].

As material, it has been used the Formlabs Rigid 4000 that is a photopolymer resin with glass reinforcement. The CAD and the manufactured wing prototype are presented in Figure 6.

Figure 6 - Wing prototype design (Bottom) and final part (top)

To perform the test, the simulacrum has been constrained to a metallic support by four screws in the front part where two specific rigid walls of 2 mm have been printed, as shown in Figure 7. These two walls fill about the 20% of the entire wing chord.

At the beginning, two piezo devices have been glued one on the top and one on the bottom external wing surface close to the support constraint to increase their bending effects (Figure 8). Then, it has been tested a second piezo configuration by adding another device into the inner wing surface as shown in Figure 7, according to the best piezo performance position of the previous configuration. The deflection of the TE has been evaluated as main target effect. The test bench used for the experiments is showed in Figure 9.

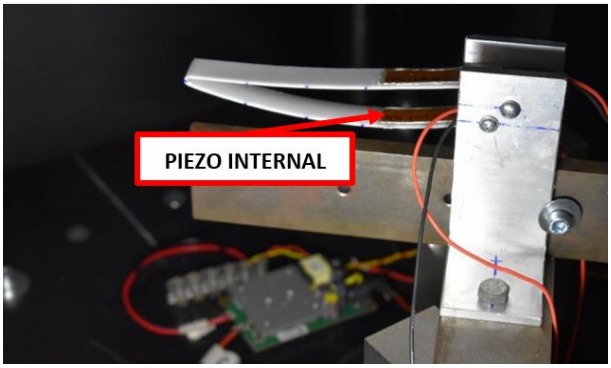

Figure 7 - Wing prototype fixture system

Piezo devices are actuated by a 12 V generator whose voltage is increased by the amplifier PI E-835 in the range of -100 V to 250 V. The input signal has been generated by a specific National Instruments module (Virtual Bench 8012) together with a MATLAB code to create square waves.

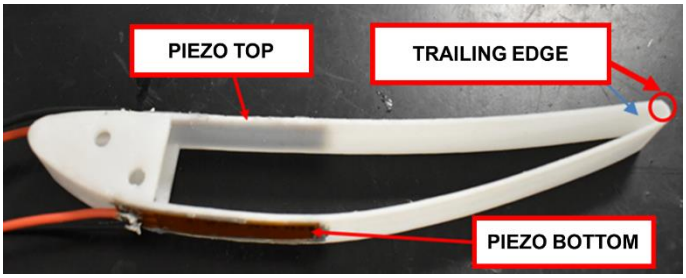

Figure 8 - Piezo positioning and TRAILING EDGE location

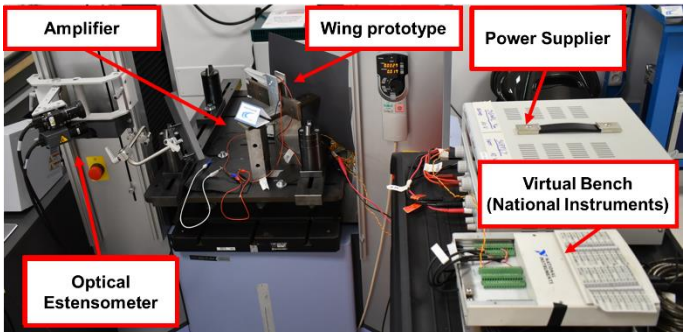

Figure 9 - EXPERIMENTAL SETUP

Different tests have been conducted to evaluate the deflection of the TE by using an optical extensometer “TRViewX” following the configuration:

Input step function between the piezo voltage operational range (-100 V and +250 V).
Input signal frequency variation between 0,2 Hz to 1 Hz by 0,2 Hz steps (Schematically represented in Figure 10).
Four repetitions for each frequency with one second of stop between every frequency cycle (Schematically represented in Figure 11).

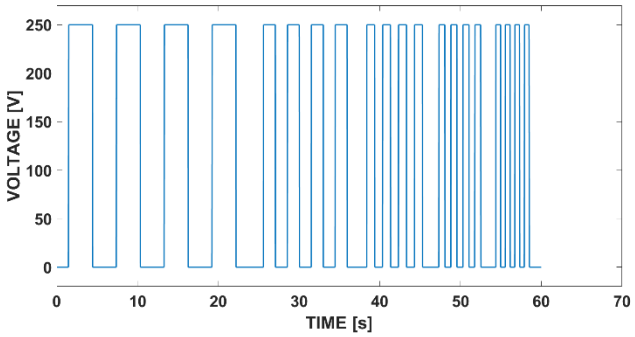

Figure 10 - Input signal: frequency variation

The first test has been conducted on both the external devices with and input step function of 0 V-250 V to investigate the maximum deflection in respect of piezo position. In Figure 12 are showed the result for the extern bottom piezo while in Figure 13 are presented the external top ones.

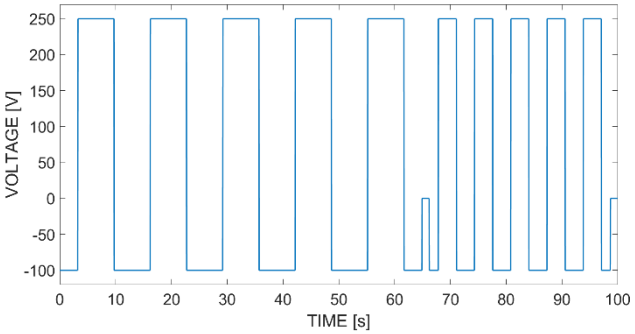

Figure 11 - Input signal: four repetitions

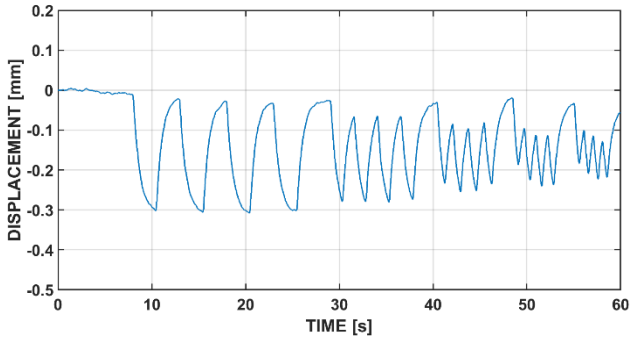

Figure 12 - Trailing Edge displacements with bottom EXTERNAL piezo actuation

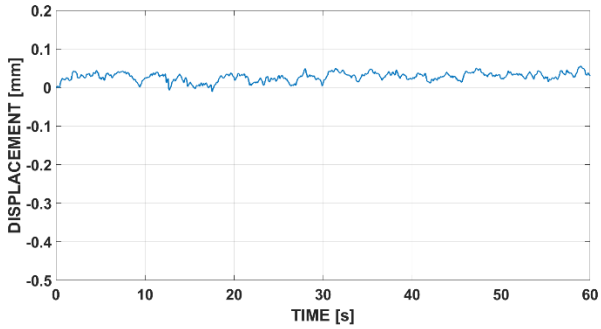

Figure 13 - TRAILING EDGE DISPLACEMENTS WITH TOP EXTERNAL PIEZO ACTUATION

Apart from this comparison another configuration was tested, using a piezo in the internal section of the wing.
To do so, it was necessary to glue yet another transducer in the wing profile. The effect of this addition is the increase of the local stiffness of the component, and it is expected that the deflection is reduced in this case.
An experiment was performed with the same characteristics previously reported and indeed the amplitude is reduced after the fixation of the new piezo Figure 14. The total reduction is as high as 50%, confirming the stiffening effect expected.

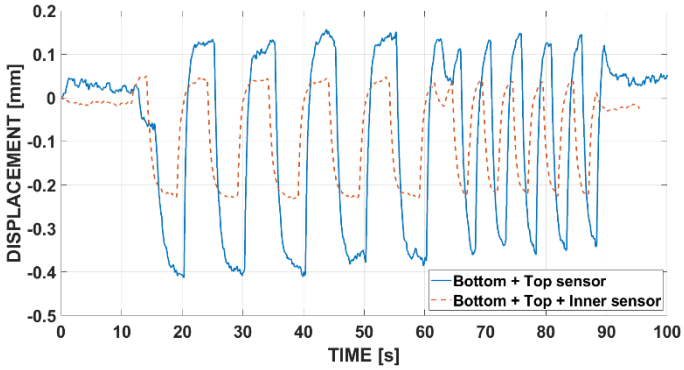

Figure 14 - DISPLACEMENT COMPARISON BEFORE AND AFTER GLUING OF INTERNAL SENSOR

Once this verification was performed, it is possible to properly compare the actuation of the internal and external surface of the bottom part of the wing. Similar inputs in terms of voltage and frequency are applied and the result for the internal zone is reported Figure 15. This analysis makes clear that the external surface is the one most suitable to the creation of high displacements.

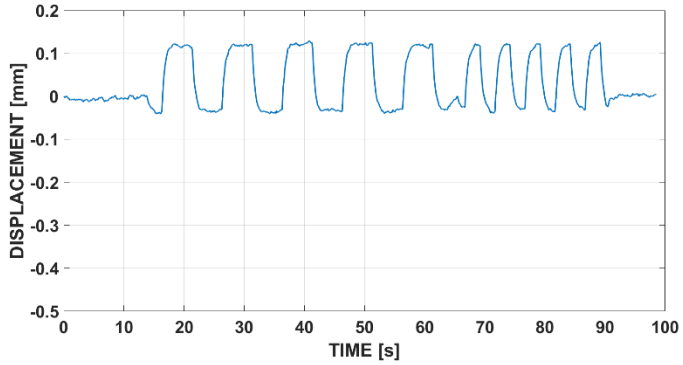

Figure 15 - TRAILING EDGE DISPLACEMENTS WITH BOTTOM INTERNAL PIEZO ACTUATION

FEM SIMULATIONs and experimental CORRELATION

The material characteristics (Table 3) were obtained through a series of traction tests executed with the same material and a fitting technique in the FEM environment.

Table 3 - Formlabs Rigid 4000 mechanical characteristics

	Tensile Strength	Young Modulus	Elongation at break
Datasheet	40 MPa	2.2 GPa	13.3 %
Experimental (Vertical)	37 MPa	2.9 GPa	24 %
Experimental (Horizontal)	32 MPa	2.7 GPa	8 %

Given that the simulations and studied phenomena are in the small displacements range, it is possible to use a linear static approach. The software used to build the model was Altair Hypermesh, and the selected solver Optistruct.

The elements of the wing section were modelled as shells, using the PSHELL elements with thickness equal to 2 mm. The bolts that connect the left and right sides of the prototype are assumed to be much stiffer than the wing section, therefore in the FEM model they are represented as rigid elements of the RBE2 type. To mimic the real degrees of freedom of the prototype all six DoF of the master nodes were blocked (Figure 16).

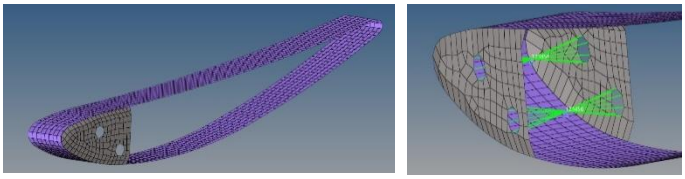

Figure 16 - Wing FEM model (left) and bolt representation (right)

The piezoelectric effect is only modelled in its active section, using elements of the 3D CHEXA type. The connection between the piezo transducers and the wing section is performed through the application of contact surfaces type FREEZE. This grants the model a perfect adhesion of the parts without slip (Figure 17).

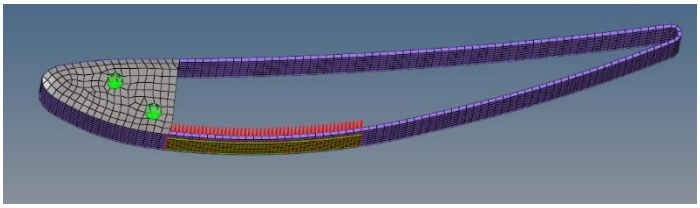

Figure 17 - FINAL FEM MODEL

To obtain a suitable representation of the piezoelectric effect, since the software interface does not have a dedicated methodology or element to do so, it was decided to use a thermal analogy. Only displacements in the longitudinal direction of the piezo transducers were considered in the analysis. In these conditions, the equations governing the phenomena can be written as:

$$\{\varepsilon_E\} = [d_{31}\, d_{32}\, d_{33}\, 0\, 0\, 0]^T \frac{\Delta V}{t}$$

$$\{\varepsilon_T\} = [\alpha_{11}\, \alpha_{22}\, \alpha_{33}\, \alpha_{23}\, \alpha_{31} \alpha_{12}]^T\, T$$

Where: ΔV is the voltage applied to the element; t represents its thickness; T is the applied temperature; and αij are the thermal coefficients.
The thermal analogy between piezoelectric effect and thermal dilatation goes as follows:

$$\begin{cases} \alpha_{11} = \dfrac{d_{31}}{t} \\ \alpha_{22} = \dfrac{d_{32}}{t} \\ \alpha_{33} = \dfrac{d_{33}}{t} \\ \alpha_{21} = \alpha_{31} = \alpha_{32} = 0 \\ T = \Delta \mathrm{V} \end{cases}$$

Table 4 shows the obtained values for the piezo-thermal correlation coefficients.

Table 4 - piezo-thermal coefficients

Piezoelectric coefficients	
$\boldsymbol{d_{31}}$ [mm/V]	-1.74 $\times 10^{-7}$

$\boldsymbol{d_{32}}$ [mm/V]	-1.74 $\times 10^{-7}$
$\boldsymbol{d_{31}}$ [mm/V]	3.94 $\times 10^{-7}$
Thermal expansion coefficients	
$\boldsymbol{\alpha_{11}}$ $[\boldsymbol{V^{-1}}]$	-8.7 $\times 10^{-7}$
$\boldsymbol{\alpha_{22}}[\boldsymbol{V^{-1}}]$	-8.7 $\times 10^{-7}$
$\boldsymbol{\alpha_{33}}[\boldsymbol{V^{-1}}]$	1.97 $\times 10^{-6}$
$\boldsymbol{\alpha_{21} = \alpha_{31} = \alpha_{32}}$	0

With these parameters set to the model, the simulation of the piezo effect can be achieved by simply applying a thermal variation between external and internal surfaces of the piezo elements. The temperature gap shall be proportional to the applied voltage, in this case a 0°C temperature applied to one side and a 250°C temperature to the other represent a 250 V voltage application. By implementing this modelling technique both to the bottom and to the top positions of the piezo transducers, the results obtained are shown in Table 5:

Table 5 - Virtual-experimental correlation on displacement

Position	Experimental	Model	Error
Top External	0.05mm	0.0445mm	10%
Bottom External	0.3mm	0.270mm	10%

virtual case study on cOMPOSITE wing

The virtual to experimental model correlation permits to consider and assume that the FEM modelling technique of piezoelectric patch is acceptable to obtain a global physical behavior of the component. Considering the range of applicability of that technology in the automotive environment, must be considered that a wing is generally been made in composite materials such as carbon fiber or glass fiber. Generally, they have higher performance respect to photopolymer used for the prototype. In fact, composite materials have an elastic modulus at least one order of magnitude more than the value of the Formlabs Rigid 4000.

Moreover, a minimum wing thickness of at least 1 mm must be considered to avoid excessive deformation due to aerodynamic effect. For these reasons, the piezoelectric patch has been actuated virtually with its maximum voltage of 1000 V to obtain a considerable deflection effect on the TE. The piezoelectric behavior will be emphasized giving higher contribution in the wing actuation, remaining in linear range.

The FE model of the composite morphing wing has the same boundary conditions and dimension of the previous one.

To achieve the maximum TE displacement guarantying a minimum wing thickness of 1mm, a structural optimization has been performed. By doing so, the wing optimized stacking sequence has been carried out. Four different composite materials have been considered:

- CT: Carbon Fiber Twill 245 g/m2
- GT: Glass Fiber Twill 380 g/m2
- CUD: Carbon Fiber Unidirectional 300 g/m2
- GUD: Glass Fiber Unidirectional 350 g/m2.

Their main characteristics are reported in Table 6. The optimization has been done considering the four materials, different composite sequence but maintaining the minimum thickness of 1 mm.

Table 6 - COMPOSITE MATERIALS MECHANICAL CHARACTERISTICS

	CT	GT	CUD	GUD
E_1 [GPa]	56	20	125	30
E_2 [GPa]	56	20	8	8
G_{12} [GPa]	3,2	2,5	3,8	3
G_{13} [GPa]	1,6	1,25	1,9	1,5
G_{23} [GPa]	3,2	2,5	3,8	3
v_{12} [GPa]	0,043	0,2	0,2	0,2

p[kg/m3]	1450	2000	1500	2000
t [mm]	0,3	0,35	0,3	0,35

From the composite optimization procedure, the solution which gives the best result is composed by 5 plies which shows a maximum displacement of the trailing edge of 0,301 mm and a total thickness of 1,35 mm (Figure 18). The stacking sequence is reported in Table 7 from the external to the internal layer.

Table 7 - optimized stacking sequence

PLY POSITION	Material	Orientation
PLY 1	GT	0°
PLY 2	CT	0°
PLY 3	CT	0°
PLY 4	CT	0°
PLY 5	CUD	90°

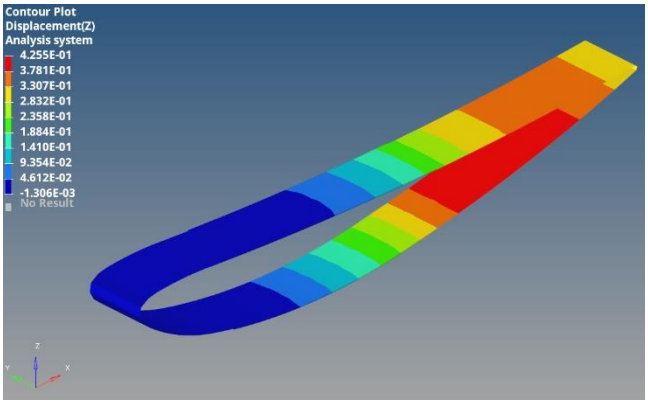

Figure 18 - DISPLACEMENT ON THE OPTIMIZED CARBON FIBER WING

Then, a simple CFD analysis has been conducted on the NACA 6412 airfoil to estimate the equivalent aerodynamic force acting on the wing. For this application, an hypotetic wing of 1500 mm length has been considered with a AOA of 6° and a fluid velocity of 100 km/h. Figure 19 reports the wing's pressure distribution contour.

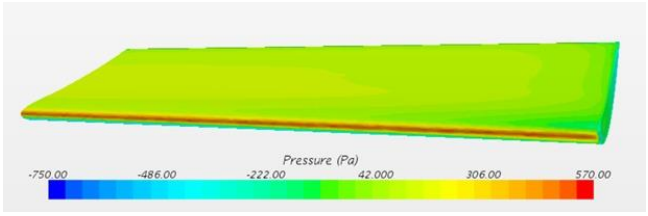

Figure 19 - Pressure distribution on NACA 6412 (AOA=6° - 100km/h)

From the pressure output acting on the airfoil, it has been carried out an equivalent force distribution considering the dimensionless ratio x/c, where "x" is the position from the leading edge and "c" is the chord line. These values have been reported in Figure 20.

.

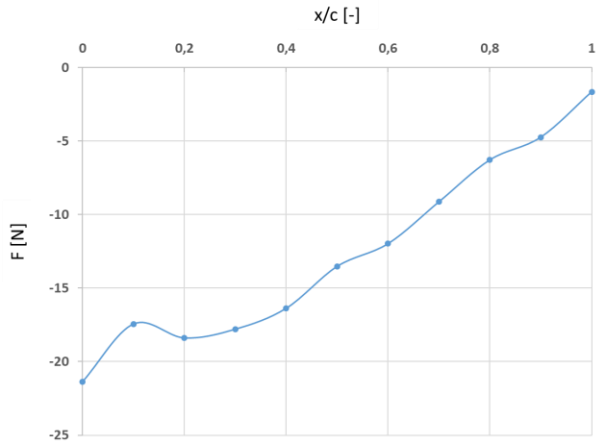

Figure 20 - Equivalent aerodynamic force distribution along the wing's chord

Subsequently, the aerodynamic forces have been scaled according to the FEM section to obtain a uniform distribution along the extrados and intrados wing nodes as shown in Figure 21.

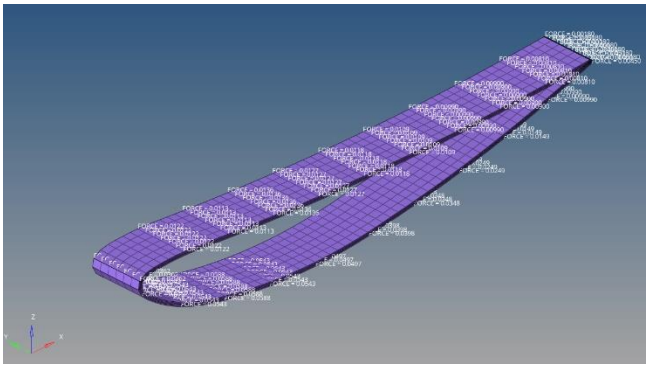

Figure 21 - Aerodynamic load applied to the wing model in FEM

Finally, a complete simulation of the morphing wing has been conducted in which it hase been considered piezo actuation and equivalent aerodynamic force simultaneously. Results depicted in Figure 22, shown a final TE displacement of -0,032 mm.

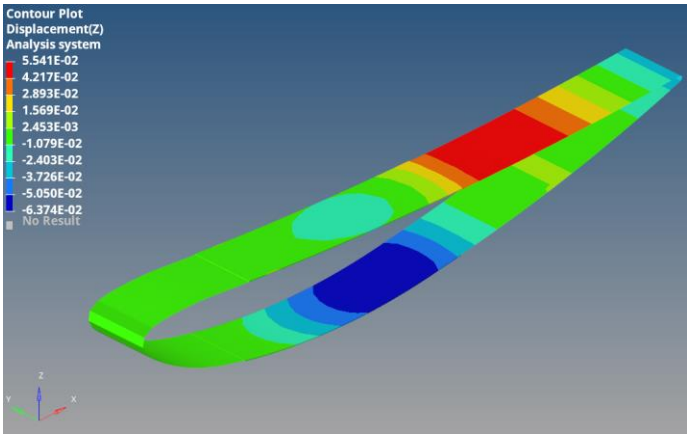

Figure 22 - DISPLACEMENTS OBTAINED WITH COMBINED PIEZO ACTUATION AND AERO LOADS

conclusion

The aim of this work is the feasibility analysis of an actuator piezo transducer for a morphing wing. For this reason, a physical simplified simulacrum has been tested to evaluate the actuation capability of this technology applied to an airfoil section.
Then, a virtual estimation of piezoelectric actuation has been simulated firstly on the simulacrum model to correlate experimental data, secondly on a composite section wing made with the same geometry. However, the obtained TE displacement remains in the order of tenth of millimeter for the considered wing section, which means angle of wing variation negligible.
These results are far from the necessary displacement of centimeters which could give a significant impact on a vehicle aerodynamic performance. Further investigations are needed to evaluate other kind of piezo solutions that could give significant contribution to active aerodynamic applications, maintaining the same advantages of lightness, thickness and composites compatibility.
Nevertheless, due to effects carried out in terms of displacement range, an interesting application could be the field of aeroacoustics control to improve NVH performances on composite components.

Acknowledgments
The authors would like to thank Luca Boaglio, Amaia Bermejo, Simone Reitano, Simone Pasini for the contribution in this work and Gianluca Poli of PI srl for piezo technology support.
References
[1] Dornoff, Jan, Miller, Joshua, Mock, Peter, and Uwe Tietge "The European Commission regulatory proposal for post-2020 CO2 targets for cars and vans: A summary and evaluation." ICCT Briefing January. (2018): https://www.theicct.org/sites/default/files/publications/ICCT_EU-CO2-proposal_briefing_20180109.pdf
[2] Ferraris, Alessandro, Micca, Federico, Messana, Alessandro, Airale, Andrea Giancarlo, and Carello, Massimiliana. "Feasibility Study of an Innovative Urban Electric-Hybrid Microcar." International Journal of Automotive Technology. Vol 20 (2019): pp.237–46. https://doi.org/10.1007/s12239-019-0023-x.
[3] Hosey, Lance. "Three Principles." The shape of green: aesthetics, ecology and design. Island Press, Washington, DC (2012): pp.37. ISBN: 978-1-61091-031-6
[4] Ferraris, Alessandro, Airale, Andrea G., Berti Polato, Davide, Messana, Alessandro, Xu, Shuang, Massai, Paolo, and Carello, Massimiliana. "City Car Drag Reduction by Means of Shape Optimization and Add-On Devices." Advances in Mechanism and Machine Science. IFToMM WC 2019. Mechanisms and Machine Science, vol 73. Springer, Cham (2019): pp.3721-3730. https://doi.org/10.1007/978-3-030-20131-9_367.
[5] Ferraris, Alessandro , De Cupis, Davide, de Carvalho Pinheiro, Henrique, Messana, Alessandro, Sisca, Lorenzo, Airale, Andrea G., and Carello, Massimiliana. "Integrated Design and Control of Active Aerodynamic Features for High Performance Electric Vehicles." SAE Technical Paper. No 2020-36-0079 (2021). doi: 10.4271/2020-36-0079.
[6] de Carvalho Pinheiro, Henrique, Russo, Francesco, Sisca, Lorenzo, Messana, Alessandro, De Cupis, Davide, Ferraris, Alessandro, Airale, Andrea G, and Carello, Massimiliana. "Advanced Vehicle Dynamics Through Active Aerodynamics and Active Body Control." Proceedings of the ASME 2020 International Design Engineering Technical Conferences and Computers and Information in Engineering Conference. Volume 4: 22nd International Conference on Advanced Vehicle Technologies (AVT). Virtual, Online. August 17–19, 2020. https://doi.org/10.1115/DETC2020-22290.
[7] de Carvalho Pinheiro, Henrique, Russo, Francesco, Sisca, Lorenzo, Messana, Alessandro, De Cupis, Davide, Ferraris, Alessandro, Airale, Andrea G., and Carello, Massimiliana. "Active Aerodynamics Through Active Body Control: Modelling and Static Simulator Validation." Proceedings of the ASME 2020 International Design Engineering Technical Conferences and Computers and Information in Engineering Conference. Volume 4: 22nd International Conference on Advanced Vehicle Technologies (AVT). Virtual, Online. August 17–19, 2020. https://doi.org/10.1115/DETC2020-22298.
[8] The Formula 1 Wiki. "Drag Reduction System". Webpage. https://f1.fandom.com/wiki/Drag_Reduction_System [Accessed Jun 14th 2021]
[9] Zenvo Automotive. "Zenvo reveals latest commission TSR-S hypercar." Webpage. Rosagervej 15, 4720 Præstø Denmark (2020). https://zenvoautomotive.com/zenvo-reveals-latest-commission-tsr-s-hypercar/ [Accessed Jun 14th 2021].
[10] FlexSys Inc. "Improving Aerodynamics." Webpage. 2205 Commonwealth Blvd, Ann Arbor, MI 48105 (2019). https://www.flxsys.com/aero [Accessed Jun 14th 2021].
[11] Debiasi, Marco T., Bouremel, Yann, Lu, Zhenbo, and Ravichandran, Varsha. "Deformation of the Upper and Lower Surfaces of an Airfoil by Macro Fiber composite actuator." Proceedings of 31st AIAA Applied Aerodynamics Conference. San Diego, CA, June 24-27, 2013. https://doi.org/10.2514/6.2013-2405
[12] Sellitto, Andrea; Riccio, Aniello. "Overview and Future Advanced Engineering Applications for Morphing Surfaces by Shape Memory Alloy Materials." Materials. 12 (5), 708 (2019). https://doi.org/10.3390/ma12050708.

[13] FlexSys Inc. “Aston Martin Incorporates FlexSys” Webpage. 2205 Commonwealth Blvd, Ann Arbor, MI 48105 (2019). https://www.flxsys.com/news/2019/3/6/flexsys-press-release-aston-martin-incorporates-flexsys-technology [Accessed Jun 14th 2021]
[14] Kochersberger, Kevin B., Osgar John Ohanian, Troy Probst, and Paul A Gelhausen. “Design and Flight Test of the Generic Micro-Aerial Vehicle (GenMAV) Utilizing Piezoelectric Conformal Flight Control Actuation.” Journal of Intelligent Material Systems and Structures 28, no. 19 (2017): pp.2793–2809. https://doi.org/10.1177/1045389X17698590.
[15] Jani, Jaronie Mohd, Leary, Martin, Subic, Aleksandar, and Gibson, Mark A. “A Review of Shape Memory Alloy Research, Applications and Opportunities.” Materials & Design. Vol. 56 (2014): pp.1078–1113. https://doi.org/10.1016/j.matdes.2013.11.084.